Stream sediment orientation survey, Aley carbonatite niobium deposit, British Columbia, Canada

Duncan A.R. Mackay[1] and George J. Simandl[1, 2]

[1]University of Victoria, School of Earth and Ocean Sciences, Victoria, BC

[2]British Columbia Ministry of Energy and Mines, Victoria, BC

Geofile 2014-05

Suggested Reference:

Mackay, D.A.R., and Simandl, G.J., 2014. Stream sediment orientation survey, Aley carbonatite niobium deposit, British Columbia, Canada. British Columbia Ministry of Energy and Mines, British Columbia Geological Survey Geofile 2014-05.

For further details please contact:

george.simandl@gov.bc.ca

Abstract:

The Aley carbonatite-hosted deposit is the most important Nb resource in the British Columbia alkaline province. Portable X-ray fluorescence (pXRF) was used effectively to determine concentrations of carbonatite pathfinder elements (Nb, Ta, La, Ce, Pr, Nd, Y, Th, U, Ba, and Sr) in stream sediments. Investigation of sediments of the unnamed creek ("AI creek") draining the Aley carbonatite area, indicates that the +250µm, +125µm, and +63µm size fractions contain high concentrations of carbonatite pathfinder elements (Nb, Ta, La, Ce, Pr, Nd, U, and Th) relative to other size fractions. The +125µm fraction was chosen for systematic evaluation of the pathfinder element distribution in AI Creek sediments because it is suitable for chemical analysis and Quantitative Evaluation of Materials by Scanning electron microscopy (QEMSCAN). The same samples enriched in pathfinder elements are expected to contain minerals characteristic of carbonatites such as pyrochlore, columbite-(Fe), fersmite, monazite-(Ce), rare earth element (REE)-bearing fluorocarbonates, barite, and apatite. Optical microscopy, electron microprobe (EMP), laser ablation inductively coupled plasma mass spectrometry (LA-ICP-MS), and QEMSCAN studies of these samples are required to identify the most useful carbonatite indicator minerals and quantify their relative abundances with increasing distance from the deposit. The main objectives of this study are to: 1) determine if stream sediment geochemistry can be used effectively to explore for Aley type deposits; 2) establish the best stream sediment size fraction for indicator minerals that might point to Nb-bearing carbonatite deposits; 3) characterize the geochemical gradient of potential pathfinder elements (Nb, Ta, REEs, P, Ba, Sr, U, and Th) in sediments downstream from the deposit, and 4) evaluate the usefulness of pXRF analyses for preliminary assessment of indicator mineral and stream sediment studies.

Introduction:

Carbonatites, carbonatite complexes, and their weathered equivalents are the main sources of Nb (Mariano, 1989a, b; Birkett and Simandl, 1999; Simandl et al., 2012, 2013a; Tantalum-Niobium International Study Center, 2013). They are most common along rift zones in intracratonic settings (Woolley and Kjarsgaard, 2008). The Aley carbonatite is one of a series of carbonatite complexes, syenite complexes, and other alkaline rocks that forms the British Columbia alkaline province (Fig. 1). It lies 135 kilometers north of Mackenzie, British Columbia and 20 kilometers northeast of the Ospika Arm of Williston Lake, east of the Rocky Mountain Trench (Fig. 1).

Geologic Setting:

The Aley carbonatite cuts Lower to Middle Paleozoic sedimentary rocks of the western Cordilleran foreland fold and thrust belt (Figs. 1, 2). The deposit is in the Cassiar terrane, which includes platformal assemblages of siliciclastic and carbonate rocks that were deposited along the western margin of Laurentia (Mäder, 1986; Pell, 1994). The Kechika Formation (Cambrian to Early Ordovician) unconformably overlies the Rosella Formation (Lower Cambrian; Pyle and Barnes, 2001). It consists of argillaceous limestone, calcareous siltstone, and dolostone. The Skoki Formation (Lower to Middle Ordovician) is generally in fault contact with the Kechika Formation and consists of dolostone and volcanic rocks (Mäder, 1986). The Road River Group (Lower to Upper Ordovician-Silurian) caps the succession, locally unconformably overlies the Skoki Formation, and consists of cherty dolostone, shale, argillaceous limestone, and rare quartzite and quartz pebble conglomerate (Mäder, 1986; Pyle and Barnes, 2001). Regional metamorphism reached lower greenschist facies (Mäder, 1986) and coincided with convergent tectonism and orogenesis between ~155 and 50 Ma (Pell, 1994; Millonig et al., 2012).

The metasedimentary sequence was intruded by the Aley carbonatite, REE-bearing carbonatite dikes, the Ospika diatreme, and lamprophyre dikes (Fig. 2; Mäder, 1986; Pell, 1994; McLeish, 2013). Zircon from the dolomite carbonate phase of the Aley carbonatite contains insufficient radiogenic Pb for U-Pb geochronology (Mäder, 1986; McLeish, 2013), but McLeish (2013) reported a U-Pb titanite age of 365.9 ± 2.1 Ma for the Ospika diatreme. The Aley carbonatite displays an early phase of deformation lacking in the Ospika diatreme indicating that it is older than ~366 Ma (McLeish, 2013). The Road River Group, (Lower to Upper Ordovician-Silurian, based on conodont biostratigraphy; Mäder, 1986; Pyle and Barnes, 2001), is the youngest unit overprinted by this early deformation that is cut by lamprophyre dikes (considered related to the Aley carbonatite and Ospika diatreme) suggesting that the Aley carbonatite is older than 366 Ma and younger than the Road River Group (McLeish, 2013).

Geology of the Aley carbonatite:

The Aley carbonatite outcrops intermittently over an area 3 to 3.5 km in diameter (Fig. 2; Mäder, 1986). It intruded sedimentary host rocks as a sill and was subsequently folded within a recumbent nappe (McLeish et al., 2010; McLeish, 2013). The main phase of the carbonatite consists of banded dolomite surrounded by minor calcite carbonatite (Mäder, 1986).The dolomite carbonatite contains apatite, pyrite, calcite, and Nb-bearing minerals such as fersmite [(Ca,Ce,Na)(Nb,Ta,Ti)$_2$(O,OH,F)$_6$], pyrochlore [(Na,Ca)$_2$Nb$_2$O$_6$(OH,F)], columbite-(Fe) [(Fe,Mn)Nb$_2$O$_6$] and rare, fine-grained acicular aggregates of Nb-rich rutile [(Ti, Nb, Fe)O$_2$]. Pods or lenses of magnetite are found throughout the dolomite carbonatite and contain apatite, phlogopite, Nb-bearing minerals, zircon, and interstitial carbonates (Kressall et al., 2010). These pods likely represent boudinaged cumulate layers. Monazite commonly co-exists with fersmite in pseudomorphs after primary columbite-(Fe) or pyrochlore (Mäder, 1986; Kressall et al., 2010).

Massive fenite surrounds the carbonatite intrusion (Fig. 2). It displays a characteristic dark blue-green colour and contains abundant richterite, arfvedsonite, and aegirine (Mäder, 1986; Kressall et al., 2010). The fenite contains brecciated metasedimentary and feldspathic material. The feldspathic breccia clasts resemble altered syenite fragments; however, they are probably strongly fenitised and albitised fragments of the Kechika Formation.

Carbonatite dikes exposed on the northwest and northeast ridges above the main deposit (Fig. 2) contain significant concentrations of light rare earth elements (LREE; Mäder, 1986). The LREE mineralization consists of REE-bearing carbonates and fluorocarbonates (Mäder, 1986). The dikes probably represent late differentiated phases of the Aley carbonatite melt (Mäder, 1986).

Geological Setting of the Aley Carbonatite

Table 1. Characteristics of stream and sample sites. Sample AL-13-09 was collected upstream of the deposit. Samples AI-13-04, AL-13-05, AL-13-06, and AL-13-07 were collected directly over the deposit. Remaining samples are in order of increasing distance downstream of the deposit.

Sample ID	Location Northing	Location Easting	Elevation (m)	Stream Character Width (m)	Depth (m)	Flow	Clast Size (cm) Average	Maximum	Dry wt. (kg)	Sample Site Characteristics
AL-13-09	6255008	425008	1408	2 to 5	0.1	Moderate	2 to 5	30	14.2	Line of fallen tree - clasts predominantly white dolomite, limestone, and slate.
AI-13-04	6256338	454355	1520	1-5	N/A	N/A	2 to 5	50	4.9	Exposed bedrock (partly covered by boulders); dry streambed; sampled from eddy between cobbles and boulders; not stained by the fenite.
AI-13-05	6256182	454349	1479	3	N/A	N/A	5 to 10	40	8.7	Dry pool below cliffs of carbonatite (Fig. 3); exposed bedrock (partly covered by boulders); not stained in the fenite.
AI-13-06	6256016	454152	1431	2	N/A	N/A	3 to 5	150	6.6	Sample from material in dry pools (<50 x 50cm) between fenite and carbonatite cobbles and boulders; not stained.
AI-13-07	6255985	454059	1400	2	N/A	N/A	2 to 5	35	6.9	Dry pool between cobbles and boulders; no exposed bedrock; sample includes large stone shape sandstone; not stained.
AI-13-08	6255181	453823	1298	3.5	0.3	rapid	5 to 10	150	9.4	Sample from matrix between cobbles and boulders (Fig. 4); predominantly slate and limestone clasts; some fenite boulders.
AI-13-02	6255244	452580	1246	3.5	0.3	rapid	5 to 10	150	14.7	Sample from matrix between cobbles and boulders; rare fenite boulders.
AI-13-10	6253666	449493	1092	4.5	0.4	rapid	5 to 10	200	14.8	Pool above bank in active channel; few of boulders; sample from matrix between cobbles and boulders; fenite and rare fenite breccia clasts are predominant.
AI-13-18	6251991	449312	928	4	0.8	rapid	1 to 2	200	12.2	Bar in a 10m↓ downstream of fallen trees; sample from matrix between cobbles and cobbles; predominantly fenite clasts; some clasts related to subcrop fenite, carbonatite, and Ospika diatreme breccia; some clasts are stained by fenite.
AI-13-18B	6251991	449314	928	4	0.8	rapid	1 to 2	200	4.1	Same as above; precipcontrite (stained to 8mm thee scatted in pam sample (blue to AL-13-18
AI-13-16	6251816	449779	891	3	0.4	rapid	2 to 5	40	14.4	5 x 10m area in lee of fallen trees, upstream of a bend
AL-13-01	6252228	443432	793	5	0.3	rapid	1 to 3	15	21.8	Lee of fallen trees.

Table 2. Relative concentrations of major and trace element analysed by factory-calibrated pXRF. Samples are listed in order of increasing distance downstream of the deposit. Concentrations in ppm except where otherwise indicated. The data are internally consistent but have not been recalibrated as described in Simandl et al. (2013b) to improve accuracy by correcting for matrix effects and biases. Based on strong positive correlation between 11 U and 15 Th pXRF, and corresponding LMB-ICPMS analyses of stream sediments from Aley, Lonnie, and Wicheeda (unpublished) processed in exactly the same manner as those in the present study, systematic overestimation of U and Th, of the order of 35% and 90% respectively, is expected. *Total Fe as ferric oxide (Fe_2O_3).

Sample	Size Fraction (µm)	Nb	Ta	Sr	La	Ce	Nd	Pr	Ba	Sr	Y	U	Th	Fe	*Fe$_2$O$_3$	% CaO
AL-13-09	+0.125	5998	117	171	1595	2538	1078	481	308	2014	180	30	570	12.88	29.34	
AL-13-09	+0.125	8647	120	156	1521	2466	1453	614	379	1659	180	32	534	12.45	27.64	
AL-13-09	+0.125	7977	123	155	1536	2447	1443	623	380	1591	180	30	497	12.96	27.06	
AI-13-04	+0.125	615	23	34	316	505	580	299	244	688	4215	8	68	3.2	26.06	
AI-13-04	+0.125	1164	24	34	316	505	580	299	244	688	4215	8	68	3.2	26.06	
AI-13-04	+2.00	728	7	38	304	491	607	303	385	304	4476	8	63	3.32	31.84	
	+2.00	585	+7	34	252	410	608	311	282	842	2788	4	70	4.03	29.99	
	+1.00	2208	65	66	545	833	777	377	297	822	5863	18	205	7.75	28.55	
	+0.500	5056	128	81	946	1402	1078	498	342	926	2894	40	451	15.08	25.42	
	+0.250	7117	153	125	1577	2410	1347	571	388	1127	4944	47	478	17.18	23.75	
	+0.125	7758	153	125	1577	2410	1347	571	388	1127	>9	44	478	11.18	23.75	
	+0.063	2429	48	71	1048	1552	827	368	374	900	9412	19	192	4.63	21.83	
	+0.063	4157	62	75	1048	1552	827	368	374	900	9412	19	192	4.63	21.83	
AL-13-10	+0.063	410	6	16	46	149	415	200	370	739	5000	2	217	1.26	22.48	
AL-13-18	+4.00	91	+7	14	166	269	442	254	407	545	560	+1	5	1.6	28.42	
	+2.00	24	+5	15	153	194	414	225	516	349	>90	1	12	1.68	25.33	
	+1.00	55	+7	16	128	209	387	219	568	352	>90	2	12	1.89	23.22	
	+0.500	97	+7	30	202	270	429	230	538	531	2292	5	88	3.34	21.8	
	+0.250	91	30	36	202	270	429	230	538	531	2292	5	88	3.34	21.8	
	+0.125	3311	78	71	662	1025	721	355	688	747	7221	28	255	6.13	21.56	
	+0.063	2258	44	62	613	1220	691	319	743	589	5224	15	177	4.44	19.7	
	-0.063	321	+7	30	273	429	408	212	552	433	>90	6	45	3.13	20.6	
AL-13-18B	+4.00	90	+7	14	166	269	442	254	407	545	>90	1	5	1.6	28.42	
	+2.00	47	+7	17	73	116	167	103	377	402	534	2	13	1.86	27.98	
	+1.00	142	+7	18	87	143	191	104	427	383	260	1	22	1.91	25.89	
	+0.500	47	+7	17	117	185	156	81	416	460	1036	4	47	2.46	23.57	
	+0.250	1412	28	42	194	302	205	108	426	583	5036	11	129	3.73	23.16	
	+0.125	2347	48	62	194	302	205	108	426	583	5036	11	129	3.73	23.16	
	+0.063	3047	48	77	613	1208	458	193	377	703	5000	27	217	4.7	22.28	
	-0.063	833	+7	36	416	814	396	187	552	491	453	9	68	2.82	23.8	
AL-13-16	+0.125	5348	101	71	1083	1648	1028	470	910	745	>90	36	355	8.55	20.98	
AL-13-01	+0.125	3495	79	72	586	936	724	346	670	711	2117	26	256	5.84	21.97	

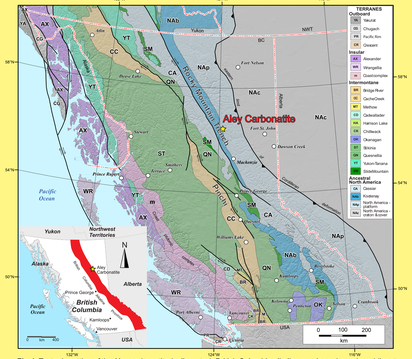

Fig.1. Tectonic setting of the Aley carbonatite (yellow star). British Columbia alkaline province shown in red (inset map). Municipalities are denoted by white circles. Modified after Colpron and Nelson (2011). Inset modified after Pell (1994).

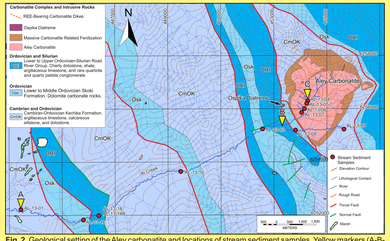

Fig. 2. Geological setting of the Aley carbonatite and locations of stream sediment samples. Yellow markers (A-B-C) denote location of profile in Fig. 5. Modified after Pride (1983), Mäder (1986), Massey et al. (2005), and McLeish (2013).

Stream Sediment Orientation Survey

Sample Collection:

Twelve stream sediment samples were collected from a creek ("AI" Fig. 2) draining the Aley carbonatite during the 2013 field season (Table 1). One sample was collected upstream of the deposit to assess background geochemistry. Four samples, spaced 200 to 300 m apart, were collected along the dry tributary of AI Creek directly over the deposit (Fig. 3a). The remaining seven samples were collected along the creek, downstream from the deposit, 1.5 to 3 km apart as access allowed (Figs. 2). The bed of the creek consists mainly of boulders, cobbles, and pebbles (Fig. 3b). Sample sites included dry pools (Fig. 3a), and the lee areas of boulders and fallen trees, and bars (Table 1). The matrix material between cobbles and boulders was sampled from an area < 1m^2 (Table 1).

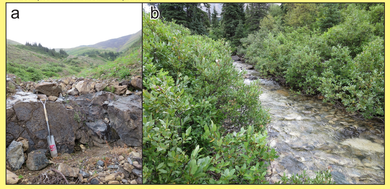

Fig. 3. Representative sample sites from the Aley carbonatite. a) AI-13-05 sample site; dry pool below chute over fenite bedrock. Sampled material forms matrix between cobbles and boulders. Looking north up the dry stream bed valley toward the deposit. Shovel is 1m long. b) AI-13-08 sample site, AI Creek, downstream of the Aley carbonatite. Sampled material constitutes matrix between cobbles and boulders, which form the predominant substrate. Stream is 3.5m wide; looking east upstream.

Portable X-ray fluorescence results:

Samples AL-13-02, AL-13-18, and AL-13-18B, were chosen for systematic study of all size fractions. High abundances of pathfinder elements (relative to other size fractions from the same samples) are observed in the +125µm size fractions for the three samples. Based on this, the +125µm fraction was chosen for systematic study. Concentrations of major oxides and trace elements (Table 2) were determined using pXRF(Thermo Fisher Scientific Niton FLX-950) following methodology in Luck and Simandl (2014). Good accuracy is expected for La and Nb. Other elements (eg. Sr) are underestimated. Remaining elements, including U and Th, are overestimated. Based on strong positive correlation between 11 U and 15 Th pXRF and corresponding LMB-ICPMS analyses of stream sediments from Aley, Lonnie, and Wicheeda (unpublished), processed in exactly the same manner as those in the present study, U and Th are overestimated of the order of 35% and 90% respectively. The pXRF is not a substitute for traditional laboratory methods where high accuracy and precision are required.

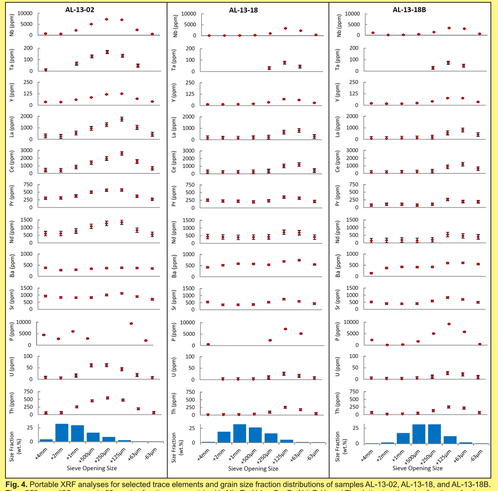

Fig. 4. Portable XRF analyses for selected trace elements and grain size fraction distributions of samples AL-13-02, AL-13-18, and AL-13-18B. The +250µm, +125µm, and +63µm size fractions are enriched in Nb, Ta, Y, La, Ce, Pr, Nd, P, U, and Th relative to other size fractions. Analyses below detection limits are not shown. Error bars based on average 2σ values determined from multiple analyses of standards by pXRF (Luck and Simandl, 2014).

Discussion:

High concentrations of Nb, Ta, La, Ce, Pr, Nd, U, and Th in the +250µm, +125µm, and +63µm fractions (Fig. 4) probably reflect the presence of carbonatite indicator minerals. The highest values coincide with the Aley carbonatite (samples AL-13-04, AL-13-05, AL-13-06; Figs. 5, 6). As expected, high concentrations of Nb, Ta, La, Ce, Y, U, Th, and Sr occur over or directly downstream of the deposit and decrease with increasing distance downstream (Figs. 5, 6; Table 2). Barium does not follow this trend, suggesting barite input from other sources. Samples taken immediately below slides (greater than 200m^2) and scree slopes (such as AL-13-07) show a decrease in the concentrations of Nb, Ta, La, Ce, Y, U, Th, and Sr relative to adjacent upstream (AI-13-06) and downstream samples (AL-13-02; Figs. 5 ,6) demonstrating the effect of dilution of pathfinder elements by incorporation of unmineralized material. Sample AL-13-02, taken in an active stream channel, has higher concentrations of pathfinder elements relative to AL-13-07 (Fig. 6), possibly due to concentration of indicator minerals by winnowing. Sample AL-13-09, obtained upstream of the Aley carbonatite (Fig. 6), has low concentrations of carbonatite pathfinder elements relative to samples downstream of the deposit. Carbonatite, fenite, and diatreme boulders immediately downstream of AL-13-18 and AL-13-18B (Figs. 5, 6; Table 2) may explain an increase in pathfinder elements in sample AL-13-16 downstream of these samples. Samples AL-13-04, AL-13-05, and AL-13-06, taken from a dry tributary (Fig. 3) of AI creek, have the highest Nb contents. This may reflect reduced levels of fluvial reworking in an intermittent stream. Alternatively, they might be the consequence of local variations in the concentration of fersmite, columbite, and pyrochlore in underlying mineralization.

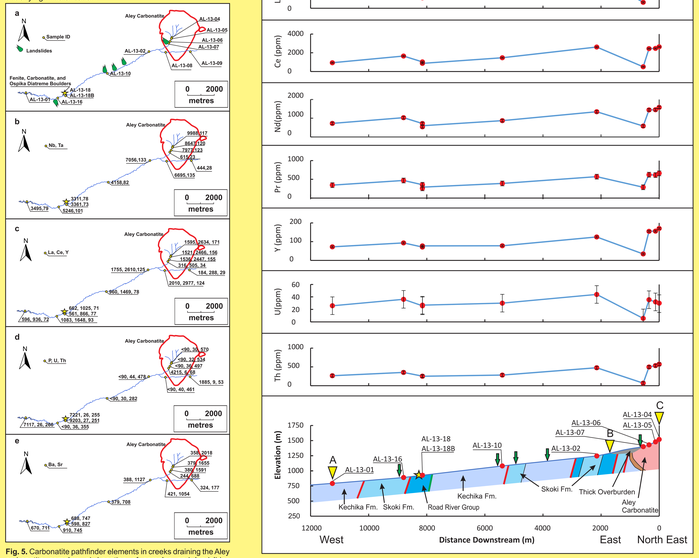

Fig. 5. Carbonatite pathfinder elements in creeks draining the Aley carbonatite complex. a) Location of samples and landslides (greater than 200m^2). b) Nb and Ta. c) La, Ce, and Y. d) P, U, and Th. e) Ba and Sr. All concentrations in ppm. Sample AL-13-07 shows the effects of significant dilution of source detritus. Sample AL-13-09 (upstream of the deposit) shows the background concentrations of trace elements.

Fig. 6. Trace elements concentrations (+125µm size fraction) in stream sediments and corresponding geological section. Concentrations of Nb, Ta, La, Ce, Y, U, Th, and Sr show a decreasing trend with increasing distance downstream of the deposit. Yellow star-fenite, carbonatite, and Ospika diatreme boulders. Green arrow-landslide/scree slope. For cross-section location see yellow markers (A-B-C) on Fig. 2. Legend for this figure is the same as in Fig. 2.

High coefficients of determination for pathfinder elements (Fig. 7) probably represent indicator mineral chemistry and mineral assemblages in stream sediments. Strong linear dependence between Nb and Fe_2O_3 (R^2 = 0.97; Fig. 7a) likely represents the co-occurrence of Nb-bearing minerals [eg. pyrochlore, columbite-(Fe), and fersmite] and magnetite or pyrite in the stream sediments. Correlation between Nb and Ta (R^2 = 0.83; Fig. 7b) agrees with the expected presence of pyrochlore, columbite-(Fe), and/or fersmite in the stream sediments. The Nb:Ta ratio of pyrochlore and columbite-(Fe) from carbonatites is typically high and is reflected in the sediments (Table 2). Niobium and La (R^2 = 0.81; Figure 7c) display a strong relationship which is likely the result of coincidence of Nb-bearing and REE-bearing minerals (REE-bearing carbonate, fluorocarbonates, and/or phosphates) in the stream sediments. Another possibility is the inclusion of REEs in the crystal structure of Nb-minerals. Poor linear dependence between Nb and TiO$_2$ (R^2 = 0.20; Figure 7d) is likely the result of low Ti concentrations expected in pyrochlore sourced from carbonatites.

Cerium correlates strongly with La (R^2 =0.99) and well with Nd (R^2 = 0.95), Pr (R^2 =0.94), and Y (R^2 =0.85). This is expected because REEs have similar physical and chemical properties and substitute for each other in the same mineral phases. Strong correlation between Ce and Th (R^2=0.90) may reflect accumulations of monazite. Zirconium correlates well with Ce (R^2 =0.95), Nd (R^2 =0.88), Pr (R^2 =0.87), La (R^2=0.86), and Y (R^2 =0.82) and may reflect its concentrations of zircon and co-occurrence with REE-bearing minerals. As expected, a significant relationship exists between Th and U concentrations (R^2=0.70).

Lack of linear dependence between Sr and Ba (R^2 =0.06) suggest that these elements are not present as a uniform barite-celestite solid solution. Sr is commonly a minor constituent of aragonite and calcite and is found in higher concentrations in REE-bearing carbonates, fluorocarbonates, and strontianite. Ba is also common in some REE-bearing carbonates, fluorocarbonates, and barite, all reported by Mäder (1986) from the Aley deposit and/or associated dikes. Barite input from non-carbonatite sources such as dolostones of Kechika and Skoki Formations is an alternative explanation.

Further optical microscopy studies combined with modern laboratory methods such as EMP, LA-ICP-MS, and QEMSCAN, will provide quantitative information on the indicator mineral signature of the Aley carbonatite deposit.

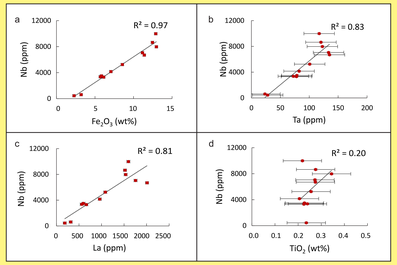

Fig. 7. Correlations between concentrations of selected pathfinder elements in the +125µm fraction of samples. a) Nb and Fe_2O_3. b) Nb and Ta. c) Nb and La. d) Nb and TiO_2.

Conclusion:

1. Stream sediment geochemistry represents a valid exploration method for Aley type carbonatite deposits using pathfinder elements such as Nb, Ta, La, Ce, Pr, Nd, Y, Th, U, and Sr.
2. The 125 to 250µm size fraction of the stream sediments is the most promising candidate for study of carbonatite related indicator minerals using QEMSCAN methods.
3. Relative concentrations of key pathfinder elements, such as Ni, Ta, La, Ce, Y, Th, U, and Sr do decrease in stream sediments downstream of the Aley carbonatite. The Ba signature of the Aley deposit, if present, is masked by other sources.
4. Based on this study and the mineralogy of the Aley deposit, pyrochlore, columbite-(Fe), and fersmite are expected to be useful indicators. Monazite, REE-bearing carbonates and fluorocarbonates, and to some extent apatite are also possible indicator minerals.
5. Additional mineralogical studies using modern laboratory methods such as EMP, LA-ICP-MS, and QEMSCAN, are in progress.

Acknowledgements:

This project received funding and support from Targeted Geoscience Initiative 4 (2010-2015), a Natural Resources Canada program carried out under the auspices of the Geological Survey of Canada. Logistical and helicopter support by Tasseko Mines Limited is greatly appreciated. Critical review by Pearce Luck (British Columbia Ministry of Energy and Mines), John Gravel (ACME Analytical Laboratories Ltd.), and Jeremy Crozier (Hunter Dickinson Inc.) greatly improved earlier versions of this manuscript. The authors would also like to thank Pearce Luck for his assistance with sample preparation and analyses.

References:

For a full list of references, please see; Mackay, D.A.R., and Simandl, G.J., 2014. Portable x-ray fluorescence to optimize stream sediment chemistry and indicator mineral surveys, case 1: Carbonatite-hosted Nb deposits, Aley carbonatite, British Columbia, Canada. In: Geological Fieldwork 2013, British Columbia Ministry of Energy and Mines, British Columbia Geological Survey Paper 2014-1, pp 183-194.